condensed matter

MDPI

Article

The EuAPS Betatron Radiation Source: Status Update and Photon Science Perspectives

Federico Galdenzi [1,2,*], Maria Pia Anania [3], Antonella Balerna [3], Richard J. Bean [4], Angelo Biagioni [3], Claudio Bortolin [3], Luca Brombal [5,6], Francesco Brun [6,7], Marcello Coreno [3,8,9], Gemma Costa [3], Lucio Crincoli [3,10], Alessandro Curcio [3], Martina Del Giorno [3], Enrico Di Pasquale [3], Gianluca di Raddo [3], Valentina Dompè [3], Sandro Donato [3,11], Zeinab Ebrahimpour [3,9], Antonio Falone [3], Andrea Frazzitta [12], Mario Galletti [1,2], Andrea Ghigo [3], Stefano Lauciani [3], Andrea Liedl [3], Valerio Lollo [3], Augusto Marcelli [3,13], Emiliano Principi [9], Andrea R. Rossi [12], Federica Stocchi [1,3], Fabio Villa [3], Marco Zottola [3], Alessandro Cianchi [1,2], Francesco Stellato [1,2,*] and Massimo Ferrario [3]

1 Dipartimento di Fisica, Università di Roma Tor Vergata, 00133 Roma, Italy; mario.galletti@lnf.infn.it (M.G.); alessandro.cianchi@roma2.infn.it (A.C.)
2 INFN-Roma "Tor Vergata", Via della Ricerca Scientifica, 00133 Rome, Italy
3 INFN-LNF, Via Enrico Fermi, 00044 Frascati, Italy; maria.pia.anania@lnf.infn.it (M.P.A.); antonella.balerna@lnf.infn.it (A.B.); angelo.biagioni@lnf.infn.it (A.B.); claudio.bortolin@lnf.infn.it (C.B.); marcello.coreno@cnr.it (M.C.); gemma.costa@lnf.infn.it (G.C.); lucio.crincoli@lnf.infn.it (L.C.); alessandro.curcio@lnf.infn.it (A.C.); martina.delgiorno@lnf.infn.it (M.D.G.); enrico.dipasquale@lnf.infn.it (E.D.P.); gianluca.diraddo@lnf.infn.it (G.d.R.); valentina.dompe@gmail.com (V.D.); sandro.donato@fis.unical.it (S.D.); zeinab.ebrahimpour@lnf.infn.it (Z.E.); antonio.falone@lnf.infn.it (A.F.); andrea.ghigo@lnf.infn.it (A.G.); stefano.lauciani@lnf.infn.it (S.L.); andrea.liedl@lnf.infn.it (A.L.); valerio.lollo@lnf.infn.it (V.L.); augusto.marcelli@lnf.infn.it (A.M.); fabio.villa@lnf.infn.it (F.V.); marco.zottola@lnf.infn.it (M.Z.); massimo.ferrario@lnf.infn.it (M.F.)
4 European XFEL GmbH, Holzkoppel 4, 22869 Schenefeld, Germany; richard.bean@xfel.eu
5 Dipartimento di Fisica, Università degli Studi di Trieste, 34127 Trieste, Italy; luca.brombal@ts.infn.it
6 INFN-Sezione di Trieste, 34127 Trieste, Italy; fbrun@units.it
7 Dipartimento di Ingegneria e Architettura, Università degli Studi di Trieste, 34127 Trieste, Italy
8 Consiglio Nazionale delle Ricerche, Istituto Struttura della Materia, LD2 Unit, 34149 Trieste, Italy
9 Elettra-Sincrotrone Trieste, Basovizza, 34012 Trieste, Italy; emiliano.principi@elettra.eu
10 Dipartimento di Fisica, University of Rome Sapienza, Piazzale Aldo Moro 5, 00185 Rome, Italy
11 Dipartimento di Fisica, Università della Calabria, 87036 Cosenza, Italy
12 INFN-Milano, Via Celoria 16, 20133 Milan, Italy; andrea.frazzitta@mi.infn.it (A.F.); andrea.rossi@mi.infn.it (A.R.R.)
13 Rome International Center for Materials Science Superstripes, 00185 Rome, Italy
* Correspondence: galdenzi@roma2.infn.it (F.G.); stellatof@roma2.infn.it (F.S.)

Abstract: The EuPRAXIA EU project is at the forefront of advancing particle accelerator research and the development of photon sources through innovative plasma acceleration approaches. Within this framework, the EuAPS project aims to exploit laser wakefield acceleration to build and operate a betatron radiation source at the INFN Frascati National Laboratory. The EuAPS source will provide femtosecond X-ray pulses in the spectral region between about 1 and 10 keV, unlocking a realm of experimental ultrafast methodologies encompassing diverse imaging and X-ray spectroscopy techniques. This paper presents a description of the EuAPS betatron source, including simulations of the photon beam parameters, outlines the preliminary design of the dedicated photon beamline, and provides an insightful overview of its photon science applications.

Keywords: free electron lasers; betatron emission; X-ray spectroscopy; phase-contrast imaging

check for updates

Citation: Galdenzi, F.; Anania, M.P.; Balerna, A.; Bean, R.J.; Biagioni, A.; Bortolin, C.; Brombal, L.; Brun, F.; Coreno, M.; Costa, G.; et al. The EuAPS Betatron Radiation Source: Status Update and Photon Science Perspective. *Condens. Matter* **2024**, *9*, 30. https://doi.org/10.3390/condmat9030030

Received: 2 May 2024
Revised: 10 July 2024
Accepted: 12 July 2024
Published: 22 July 2024

1. Introduction

The European Plasma Research Accelerator with eXcellence In Applications (EuPRAXIA) project aims to develop particle accelerator research infrastructures based on

novel plasma acceleration concepts and laser technology [1]. One of the key elements of plasma acceleration is the so-called driver pulse, which creates a wakefield in plasma that is then exploited to accelerate electron bunches. The driver pulse can be either a laser, leading to a Laser Wakefield Accelerator (LWFA) [2–5], or charged particles (such as electrons), or a pulse, leading to a Particle Wakefield Accelerator (PWFA). Betatron radiation is the characteristic emission of photons originating from electrons traveling along an oscillatory path at relativistic speeds, as happens in LWFA or PWFA. This betatron radiation, exhibiting a certain level of coherence, is emitted within a narrow forward cone with a source size typically of a few microns and exhibits a relatively high level of transverse coherence. The photon pulse duration is comparable to the duration of the driver pulse and therefore falls in a timescale of femtoseconds. The short duration of the pulses results in a peak brilliance comparable with that of synchrotron sources, although with a lower repetition rate, typically Hz, as compared to MHz for synchrotrons. Betatron sources' pulses carry fewer photons than FELs (e.g., [6]) but with a similar pulse length and transverse coherence characteristics. The energy spectrum is broad, like that of a wiggler synchrotron radiation source with comparable peak brilliance. Betatron sources can be considered between free electron laser (FEL) sources and synchroton radiation sources, with the short pulse and coherence of FELs but broad energy range of synchrotrons, as we can see in Figure 1, where we compared expected peak brilliance with that of betatron sources around the world.

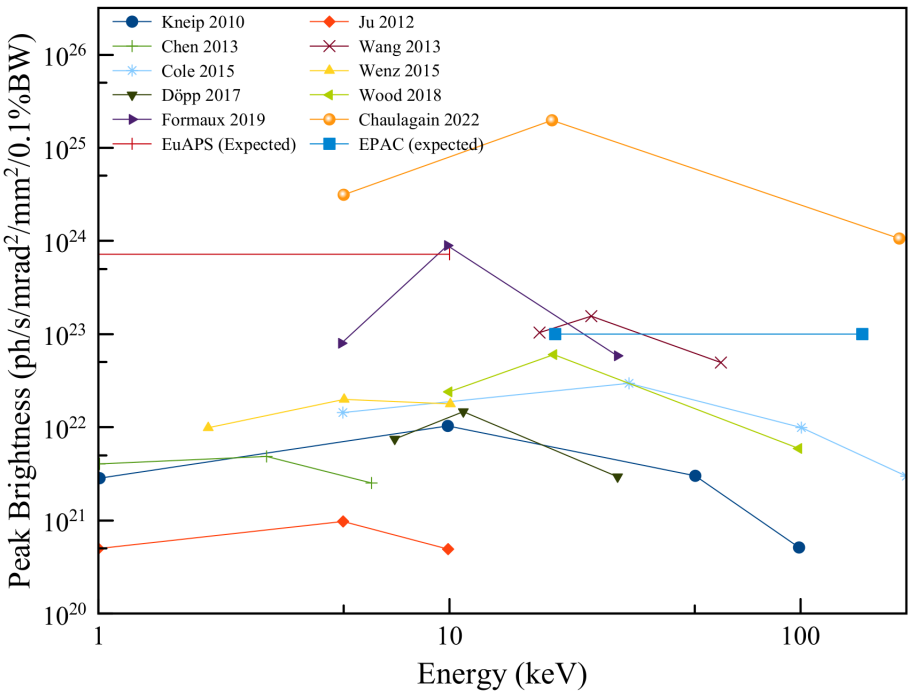

Figure 1. Peak brightness for different betatron X-ray sources [6–15] compared to the expected one from EuAPS. The EPAC laser-plasma source is expected to have a brilliance greater than 10^{23}. All the other data in this figure were extrapolated from Chaulagain et al. [6].

The main advantages of betatron sources concerning synchrotrons and FELs are their compactness and lower cost. The ultimate goal of EuAPS is to operate a stable, compact, ultra-fast X-ray source that can reduce the economic and environmental impact of large photon radiation facilities without losing their capabilities [16]. In this paper, we provide a description of the EuAPS betatron source parameters based on simulations, present an outline and a preliminary design of the dedicated photon beamline, and give an overview of the foreseen applications.

2. Results

2.1. Simulations

Preliminary simulations on the energy spectrum and intensity of the betatron radiation have been presented in Ref. [17]. Here, we provide updated figures taken from the simulations reported in Ref. [18], which were performed exploiting a model based on a particle-in-cell (PIC) data structuring process. This method, which chooses a specific set of particles, is based on their position and momentum and collects data related to this set at any point in time [19]. Position, moments, and electrical fields obtained from these calculations are then used to perform parallel calculations of the produced electric fields. The dynamics of the electrons and the emitted radiation have been calculated separately due to the significant difference in energy scales; electron energies are on the order of 100 MeV, while single-photon energies are 1–10 keV. The Fourier transform of the computed total field allows radiation spectrum retrieval. All the specifications of the simulations are reported in Ref. [18], where the code is explained in more depth and is tightly connected to our work. All the parameters of the simulation are contained in Table 1. The driver laser source is the FLAME femtosecond laser system, which is able to provide pulses with a maximum energy of 7 J, temporally compressed down to 25 fs, with a peak power of 200 TW and 10 Hz repetition rate. To give an overview of possible scenarios, the simulations are repeated for three different plasma densities achievable at EuAPS.

Table 1. Parameters of the simulations and—in the last row—corresponding photon beam parameters.

Laser Energy [J]	2.5
Plasma Density [cm^{-3}]	1.7×10^{18}
Beam Energy [MeV]	395
Transverse beam size RMS [μm]	1.5
Charge [pC]	144
Pulse Duration [fs]	25
Photons @ energy per pulse > 1 keV	1.7×10^{9}

The main outcome of the simulations is that considering the plasma densities achievable at EuAPS, the expected number of photons/pulse with energy > 1 keV is on the order of 10^9 photons/pulse. The simulations allowed us to estimate the X-ray beam profiles that we expect to obtain. The simulations were carried out following the data obtained from the PIC models and a gas mixture of He-N_2. We started from pure helium gas and added integer percentages of N_2 into the mixture up to 5%. The results are shown in Figure 2, with spots of the simulated betatron radiation with mixtures from 0% nitrogen to 5%.

Despite the fidelity of the simulations, other studies have noted that betatron radiation's properties are prone to fluctuation due to the nature of the generation process [12,20]. Experimental data for the X-ray beam profile have shown that the beam shape generated from pure helium (the most common type of gas used) has very asymmetrical features that are highly dependent on the stability of the emission [12].

2.2. Experimental Chamber

As reported above, the main foreseen applications of the EuAPS photon beam will be X-ray imaging and spectroscopy. To also perform experiments in the low range of the energy spectrum, where air absorption would be consistent, EuAPS foresees the installation of a high-vacuum experimental chamber. Here, we describe the design of the experimental chamber that will allow us to perform increasingly complex experiments, starting from imaging measurements, but keeping the possibility of performing X-ray spectroscopy experiments. The chamber has a rectangular base of 0.8 m × 3 m and is 0.8 m high. It is composed of three different modules (as shown in Figure 3), and it is capable of

reaching a pressure of 10^{-6} mbar. The betatron beam, generated in a dedicated gas-jet chamber located upstream from the experimental chamber, enters the experimental chamber through a dedicated flange. The side panels of the modules have five flanges allowing the coupling with external lasers for pump-probe experiments, the installation of other devices, and easing access to the chamber.

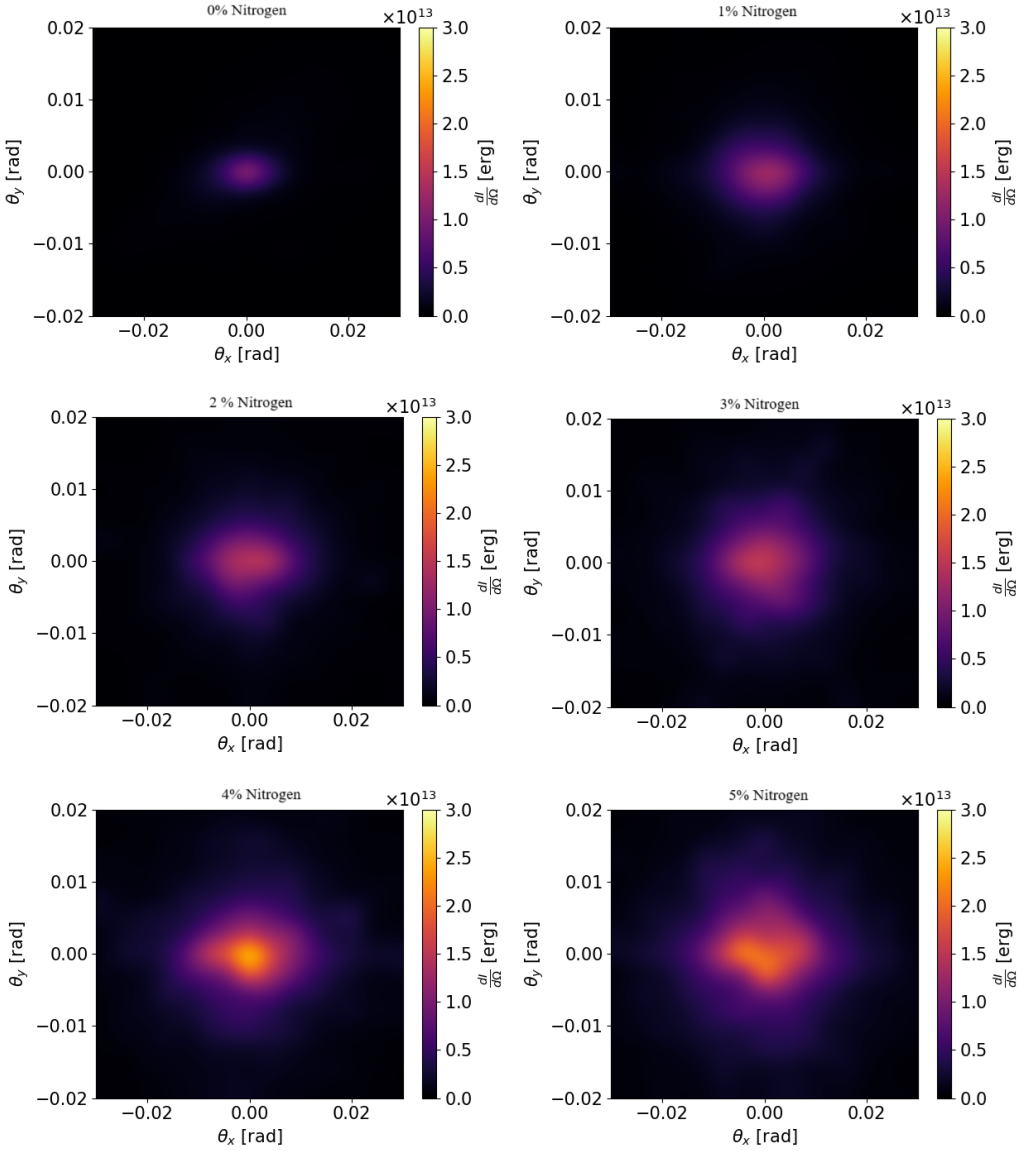

Figure 2. X-ray beams spot simulation obtained from the PIC method explained in the text. The spot was simulated starting from a 0% addition of N_2 to the He gas of up to 5% of N_2 in the mixture. We can see that the N_2 gas added to the mixture enhances the intensity of the beam in the 10 millirad range around the center, without affecting the shape. However, this enhancement rapidly falls off at 5% mixture. The energy range of the simulations is between 1 and 10 keV.

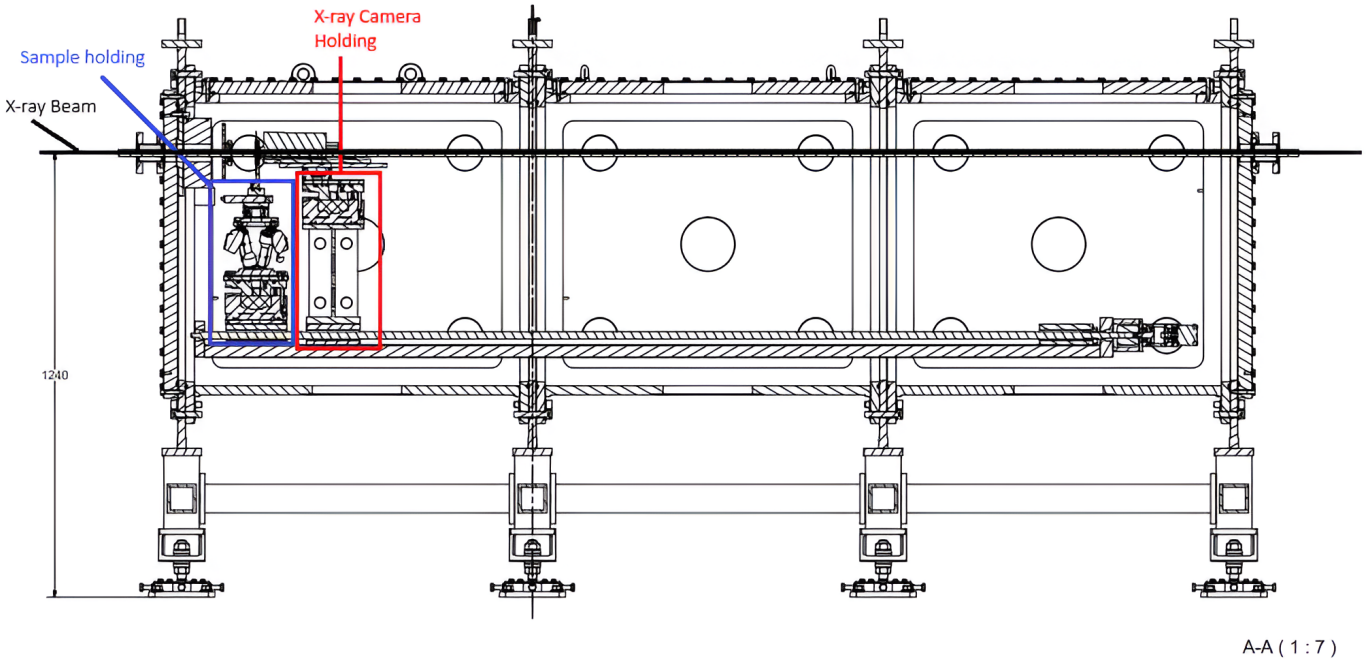

Figure 3. CAD schematic of the Experimental Chamber that has been described in the text. The X-ray beam, the sample holding system, and the X-ray camera holding system are highlighted. At the bottom of the chamber, the 2.5 m rail system can be seen.

In its initial setup, the experimental chamber will be equipped with a 2.5 m linear rail, where a CCD X-ray camera and the sample holder will be mounted. The camera will be a PI-MTE3 Teledyne back-illuminated 2048 × 2048 pixel CCD camera with a pixel size of 15 × 15 μm^2. At the beam entrance, a motorized X-ray slit and a filter wheel capable of holding six different X-ray filters of sufficient size (2 inches/5.08 cm) will be installed to interact with the full beam. A first XYZ stage will be used for sample alignment, and then two linear stages will allow the sample holder to move in the XY plane (parallel to the ground) while a rotating stage will be used to rotate the sample holder 360° around the z-axis (perpendicular to the ground). A hexapod will be used to move the sample holder in the XYZ direction and to optimize the sample position in relation to the CCD camera. The CCD camera alignment system, placed on the linear rail, will be positioned at the optimal distance from the sample for X-ray imaging purposes (the equipment disposition is represented in Figure 4).

It is worth pointing out that the chamber will be large enough to accommodate other pieces of instrumentation, like crystal-based optical components and extra radiation detectors, which will be needed to perform X-ray spectroscopy experiments. This ensures that the chamber will be flexible enough to follow possible evolution and improvements of the betatron source, as pointed out above.

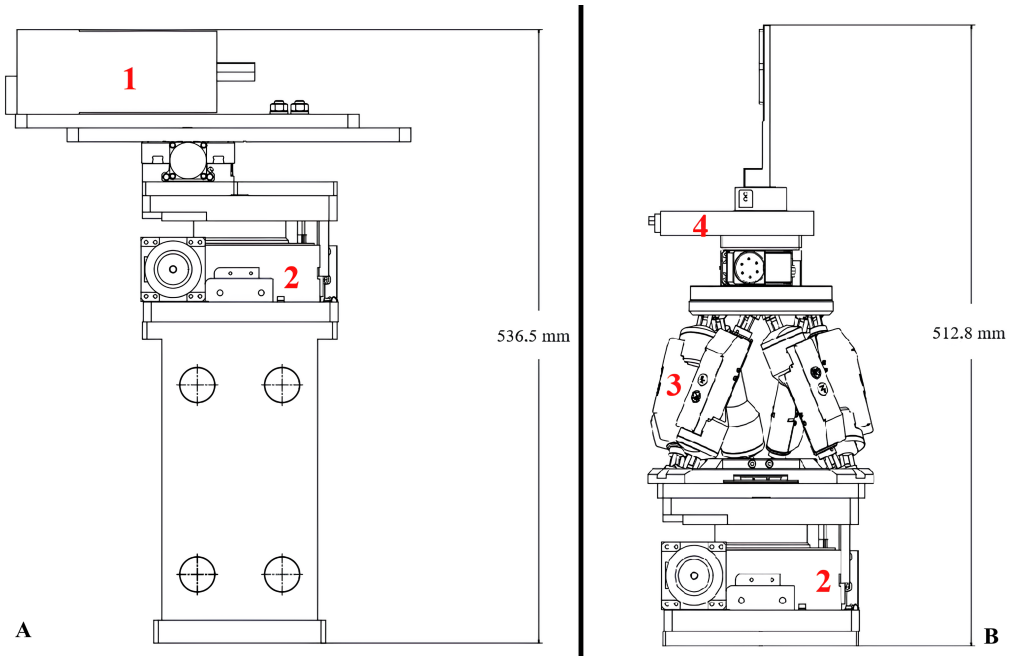

Figure 4. Particular of the camera system (panel **A**) and the sample system (panel **B**) that will be installed in the EuAPS chamber. In red, (1) is the X-ray CCD camera (PI teledyne, 2048 × 2048 res, 15 µm pixel size, 30.7 × 30.7 mm size), (2) represents the two z-linear stages, (3) is the hexapod, and (4) is the sample alignment system composed of 2 linear stages and 1 rotary stage, all under the sample holder plate. All components are high-vacuum-compatible.

3. Discussion

Some possible applications of the betatron photon beam at LNF have already been described in a previous article [17]. Here, taking into account the substantial financial support granted by the NextGenerationEU program, and the latest results on the expected source parameters, we provide an updated and more detailed photon science plan compatible with the design of the experimental setup described in Section 2.2. The timeline foresees the source to be operational in 2025 and to remain active for at least 10 years after the end of construction.

Other works have demonstrated that the stability and quality of the beam can be improved with the use of an ionization-injection regime (e.g., Refs. [12,21]) that will be implemented in our facility. The idea is therefore to start with a pilot experiment and to increase the number and complexity of applications while improving the source at the same time. In the following paragraphs, we describe the main classes of experiments foreseen for the EuAPS source, namely X-ray imaging and X-ray spectroscopy, following the scheme presented in Table 2.

Table 2. Main classes of experiments to be performed at the EuAPS betatron source. In the first column, the priority index corresponds to the hierarchy of the experiments in the EuAPS timeline. The second column lists the experimental techniques and specifies whether the experiments are static or time-resolved. The last column summarizes the foreseen types of samples

Priority	Technique	Samples
1	Static CT and PCI	Leaves, wood, insects, animal tissues, ancient papers
2	Static XAS	Metal foils
3	Time-resolved XAS	Metal foils, nanoparticles
4	Time-resolved imaging	Bulk materials, liquid jets, plasmas, sprays

3.1. Imaging

X-ray imaging is routinely performed by exploiting various X-ray sources, from conventional X-ray tubes to accelerator-based facilities. Conventional X-ray imaging is based on the detection of variations in the X-ray attenuation coefficient within the sample. This principle is routinely used to obtain bi-dimensional, i.e., radiography, and three-dimensional, i.e., computed tomography, representation of the scanned object. However, light materials, such as soft tissues, feature a poor attenuation contrast and are therefore hardly visible through attenuation-based imaging [22]. Owing to the high lateral coherence of the betatron source, X-ray phase-contrast imaging (PCI) techniques can be implemented, offering a much higher sensitivity to light materials. PCI enables the visualization of phase effects, which are dependent on the phase shift experienced by the X-rays traversing the sample. PCI has already shown its potential at betatron radiation sources to image biological objects, such as tissues and small organisms [11,23–26] and inorganic materials [27].

The photon flux achievable by the EuAPS source, which is on the order of 10^9 photons/pulse, can allow aiming at micron resolution with single-shot measurements [28,29]. The EuAPS pilot experiment will be aimed at studying samples for which a resolution of some microns will be sufficient to yield valuable information. In this context, the imaging of highly structured samples of biological samples, such as vegetables (e.g., Ref. [30]) or soft-tissue biological samples, will be the first application to be developed. Thanks to the broad spectral range emitted by the source, spectral imaging can be achieved by adjusting the shape and average energy of the spectrum using suitable filters made of various materials placed between the source and the sample. Repeated acquisitions of the same sample with varying spectra can allow the identification of specific elements, such as the presence of heavy metals. This scheme, for instance, could be used to study the distribution of pollutants in the samples. Other foreseen applications of PCI at EuAPS include non-destructive imaging of cultural heritage samples, such as ancient documents. Again, the strategy of applying filters to obtain elemental sensitivity will be a key point to clearly distinguish the presence of different inks, therefore allowing a virtual reading of otherwise impossible-to-access documents [31–33]. Moreover, among the different PCI techniques, Edge Illumination (EI) beam-tracking (BT) [34–37] is one of the most promising phase-contrast imaging-based approaches for experiments at betatron sources. This technique is based on the tracking, at a pixel-by-pixel level, of the changes introduced by the sample upon a structured illumination field, which is created through a periodic absorbing structure positioned upstream from the sample. With this technique, Doherty et al. [30] obtained multimodal images, in transmission, refraction, and scattering, with both single-shot and multiple-shot modes using a betatron source with parameters similar to EuAPS. The most important condition for good BT/EI images is to have a small camera pixel size (<15 μm), but it relaxes the requirements in terms of spatial coherence. In the framework of the EuAPS project, EI will represent the first test to show the capability of the betatron source to encode multiple information with a single-shot acquisition approach. The further steps in imaging at EuAPS will be exploiting the pulsed nature of the betatron source to perform time-resolved imaging measurements. Potential applications include imaging of sprays [38] and ultrafast phenomena, such as the propagation of laser-driven shock-waves in materials, which can be tracked with a resolution down to tens of femtoseconds [13].

3.2. X-ray Spectroscopy

While more demanding from the instrumentation point of view than imaging, X-ray spectroscopy can benefit from the characteristics of betatron radiation sources [39]. Indeed, its wide energy range makes it suitable for X-ray absorption spectroscopy (XAS) experiments, both in the X-ray absorption near-edge spectroscopy (XANES) and in the extended X-ray absorption fine structure (EXAFS) energy regions [40–42], and its pulsed structure allows performing time-resolved experiments. Methods and potentialities for time-resolved XAS have been demonstrated at pulsed sources such as FELs in the last decade and are becoming more and more widespread [43–45]. It is worth pointing out that,

to date, betatron sources are the only ones emitting femtosecond pulses with a broad energy spectrum. For this reason, they are the best candidates to perform time-resolved measurements in the EXAFS region, which requires a range of a few hundred eV. For samples in which the cross-section is large—and therefore allows achieving a good signal-to-noise ratio—a photon flux as high as the FELs one is not necessary, and the much smaller and less expensive betatron sources can be used instead. For this reason, betatron XAS experiments have been so far mainly used to study metallic samples or other bulk materials. To maximize the flux on the sample, XAS at betatron sources is typically performed in dispersive mode, with curved or mosaic crystal analyzers focusing the white beam on the sample and position-sensitive detectors measuring the transmitted intensity. The advantage of this scheme is that no monochromator is needed, and so all the photons emitted by the source reach the sample. Pump-probe XAS experiments on copper [40] and aluminum [46] demonstrated the potential of betatron XAS to study non-equilibrium phenomena. XAS experiments at the betatron can also be performed in single-shot mode. Kettle et al. [47] showed that it is possible to obtain single-shot K-edge XANES spectra of a titanium sample with a betatron radiation source with 10^6 photons/eV in the 5 keV region, with a signal-to-noise ratio of 300:1. The same group successfully acquired EXAFS data from a copper foil [48] exploiting single shots of a betatron source delivering photons at 0.05 Hz. These works pave the way for single-shot time-resolved XAS experiments.

As pointed out in Section 2.2, the EuAPS experimental chamber is large enough to accommodate the instrumentation needed to perform XAS experiments, in both static and time-resolved mode. In particular, following Mahieu et al. [40], we plan to install a setup where a toroidal mirror is used to focus the X-ray beam on the sample and a toroidal crystal deviates the transmitted beam on the CCD. While toroidal mirrors are a direct and relatively easy solution to deliver the photon beam to the experimental stations, they have low efficiency and are difficult to align. For these reasons, in a second stage, we will install a Multi-Lane mirror system, as described by Raclavsky et al. and Zerauli et al. [49,50], with a broad range of applications that would highly speed up all the alignments and, at the same time, have higher efficiency in delivering the beam. Given the expected photon count of EuAPS, the first XAS experiments will be performed in the XANES region, which is characterized by a higher signal-to-noise level with respect to the EXAFS. Oscillations in the EXAFS are indeed generally about 1% of the edge step in amplitude [51], while XANES and its oscillations can be as intense as the edge step [52]. Performing the first XAS experiments on metallic samples (due to the higher cross-section than lighter elements) in the XANES region will therefore be the initial phase of the spectroscopy program at EuAPS. A list of EuAPS applications, in order of priority, is given in Table 2.

It is also worth pointing out that, thanks to the higher repetition rate of the EuAPS source (1 Hz at the start of the betatron source life) concerning the aforementioned XAS experiments (0.05 Hz), it will be possible to acquire more spectra within the same time. This is particularly relevant for pump-probe experiments, in which the samples are first pumped by an intense femtosecond laser and then probed by the X-ray betatron pulse coming with an appropriate delay. These experiments indeed require the collection of a full spectrum for each delay and therefore are more time-consuming than static experiments.

Author Contributions: Conceptualization, F.G. and A.C. (Alessandro Cianchi); Investigation, F.G., A.F. (Andrea Frazzitta), V.L., A.R.R. and F.S. (Francesco Stellato); Validation, F.G., M.P.A., A.B. (Antonella Balerna), R.J.B., A.B. (Angelo Biagioni), C.B., L.B., F.B., M.C., G.C., L.C., A.C. (Alessandro Curcio), M.D.G., E.D.P., G.d.R., V.D., S.D., Z.E., A.F. (Antonio Falone), M.F., A.F. (Andrea Frazzitta), M.G., A.G., S.L., A.L., V.L., A.M., E.P., A.R.R., F.S. (Federica Stocchi), F.V., M.Z., A.C. (Alessandro Cianchi) and F.S. (Francesco Stellato); Writing—original draft, F.G.; Writing—review and editing, F.G., A.B. (Antonella Balerna), Z.E., A.M., E.P., A.C. (Alessandro Cianchi) and F.S. (Francesco Stellato). All authors have read and agreed to the published version of the manuscript.

Funding: This work was funded by the European Union under the Horizon Europe grant EuPRAXIA-PP (Grant Agreement No. 101079773) and by European Union—NextGeneration EU. Francesco Stellato and Richard J. Bean acknowledge financial support from the Italian Ministry for Foreign

Affairs and International Cooperation (FELIX project). Francesco Stellato acknowledges financial support from the University of Rome Tor Vergata (PANDA project) and from INFN (BIOPHYS).

Data Availability Statement: The raw data supporting the conclusions of this article will be made available by the authors on request.

Conflicts of Interest: Richard J. Bean was employed by the European XFEL GmbH. The authors declare no competing financial interest.

Abbreviations

The following abbreviations are used in this manuscript:

CT	Computer Tomography
EuAPS	EuPRAXIA Advanced Photon Sources
EXAFS	Extended X-ray Absorption Fine Structure
FLAME	Frascati Laser for Acceleration and Multidisciplinary Experiments
INFN	Istituto Nazionale di Fisica Nucleare
LNF	Laboratori Nazionali di Frascati
LWFA	Laser Wakefield Accelerator
PCI	Phase Contrast Imaging
PWFA	Particle Wkefield Accelerator
XANES	X-ray Absorption Near Edge Spectroscopy
XAS	X-ray Absorption Spectroscopy

References

1. Assmann, R.; Weikum, M.; Akhter, T.; Alesini, D.; Alexandrova, A.; Anania, M.; Andreev, N.; Andriyash, I.; Artioli, M.; Aschikhin, A.; et al. EuPRAXIA conceptual design report. *Eur. Phys. J. Spec. Top.* **2020**, *229*, 3675–4284.
2. Rakowski, R.; Zhang, P.; Jensen, K.; Kettle, B.; Kawamoto, T.; Banerjee, S.; Fruhling, C.; Golovin, G.; Haden, D.; Robinson, M.S.; et al. Transverse oscillating bubble enhanced laser-driven betatron X-ray radiation generation. *Sci. Rep.* **2022**, *12*, 10855. [CrossRef] [PubMed]
3. Kozlova, M.; Andriyash, I.; Gautier, J.; Sebban, S.; Smartsev, S.; Jourdain, N.; Chaulagain, U.; Azamoum, Y.; Tafzi, A.; Goddet, J.P.; et al. Hard X Rays from Laser-Wakefield Accelerators in Density Tailored Plasmas. *Phys. Rev. X* **2020**, *10*, 011061. [CrossRef]
4. Lamač, M.; Chaulagain, U.; Jurkovičová, L.; Nejdl, J.; Bulanov, S. Two-color nonlinear resonances in betatron oscillations of laser accelerated relativistic electrons. *Phys. Rev. Res.* **2021**, *3*, 033088. [CrossRef]
5. Zhao, T.; Behm, K.; Dong, C.; Davoine, X.; Kalmykov, S.Y.; Petrov, V.; Chvykov, V.; Cummings, P.; Hou, B.; Maksimchuk, A.; et al. High-flux femtosecond X-ray emission from controlled generation of annular electron beams in a laser wakefield accelerator. *Phys. Rev. Lett.* **2016**, *117*, 094801. [CrossRef] [PubMed]
6. Chaulagain, U.; Lamač, M.; Raclavskỳ, M.; Khakurel, K.; Rao, K.H.; Ta-Phuoc, K.; Bulanov, S.; Nejdl, J. ELI gammatron beamline: A dawn of ultrafast hard X-ray science. *Photonics* **2022**, *9*, 853 [CrossRef]
7. Ju, J.; Svensson, K.; Döpp, A.; Ferrari, H.E.; Cassou, K.; Neveu, O.; Genoud, G.; Wojda, F.; Burza, M.; Persson, A.; et al. Enhancement of X-rays generated by a guided laser wakefield accelerator inside capillary tubes. *Appl. Phys. Lett.* **2012**, *100*, 191106 . [CrossRef]
8. Chen, L.; Yan, W.; Li, D.; Hu, Z.; Zhang, L.; Wang, W.; Hafz, N.; Mao, J.; Huang, K.; Ma, Y.; et al. Bright betatron X-ray radiation from a laser-driven-clustering gas target. *Sci. Rep.* **2013**, *3*, 1912. [CrossRef]
9. Wang, X.; Zgadzaj, R.; Fazel, N.; Li, Z.; Yi, S.; Zhang, X.; Henderson, W.; Chang, Y.Y.; Korzekwa, R.; Tsai, H.E.; et al. Quasi-monoenergetic laser-plasma acceleration of electrons to 2 GeV. *Nat. Commun.* **2013**, *4*, 1988. [CrossRef]
10. Cole, J.; Wood, J.; Lopes, N.; Poder, K.; Abel, R.; Alatabi, S.; Bryant, J.; Jin, A.; Kneip, S.; Mecseki, K.; et al. Laser-wakefield accelerators as hard X-ray sources for 3D medical imaging of human bone. *Sci. Rep.* **2015**, *5*, 13244. [CrossRef]
11. Wenz, J.; Schleede, S.; Khrennikov, K.; Bech, M.; Thibault, P.; Heigoldt, M.; Pfeiffer, F.; Karsch, S. Quantitative X-ray phase-contrast microtomography from a compact laser-driven betatron source. *Nat. Commun.* **2015**, *6*, 7568. [CrossRef]
12. Döpp, A.; Mahieu, B.; Lifschitz, A.; Thaury, C.; Doche, A.; Guillaume, E.; Grittani, G.; Lundh, O.; Hansson, M.; Gautier, J.; et al. Stable femtosecond X-rays with tunable polarization from a laser-driven accelerator. *Light. Sci. Appl.* **2017**, *6*, e17086. [CrossRef] [PubMed]
13. Wood, J.; Chapman, D.; Poder, K.; Lopes, N.; Rutherford, M.; White, T.; Albert, F.; Behm, K.; Booth, N.; Bryant, J.; et al. Ultrafast imaging of laser driven shock waves using betatron X-rays from a laser wakefield accelerator. *Sci. Rep.* **2018**, *8*, 11010. [CrossRef]
14. Fourmaux, S.; Hallin, E.; Arnison, P.; Kieffer, J. Optimization of laser-based synchrotron X-ray for plant imaging. *Appl. Phys. B* **2019**, *125*, 34. [CrossRef]

15. Sims, M. EPAC X-ray Radiography and X-ray Computed Tomography. Available online: https://www.clf.stfc.ac.uk/Pages/EPAC-X-Ray-radiography-and-X-ray-Computed-Tomography.aspx (accessed on 11 July 2024).
16. Emma, C.; Van Tilborg, J.; Assmann, R.; Barber, S.; Cianchi, A.; Corde, S.; Couprie, M.; D'arcy, R.; Ferrario, M.; Habib, A.; et al. Free electron lasers driven by plasma accelerators: Status and near-term prospects. *High Power Laser Sci. Eng.* **2021**, *9*, e57. [CrossRef]
17. Stellato, F.; Anania, M.P.; Balerna, A.; Botticelli, S.; Coreno, M.; Costa, G.; Galletti, M.; Ferrario, M.; Marcelli, A.; Minicozzi, V.; et al. Plasma-Generated X-ray Pulses: Betatron Radiation Opportunities at EuPRAXIA@ SPARC_LAB. *Condens. Matter* **2022**, *7*, 23. [CrossRef]
18. Frazzitta, A.; Bacci, A.; Carbone, A.; Cianchi, A.; Curcio, A.; Drebot, I.; Ferrario, M.; Petrillo, V.; Conti, M.R.; Samsam, S.; et al. First Simulations for the EuAPS Betatron Radiation Source: A Dedicated Radiation Calculation Code. *Instruments* **2023**, *7*, 52. [CrossRef]
19. Lehe, R.; Kirchen, M.; Andriyash, I.A.; Godfrey, B.B.; Vay, J.L. A spectral, quasi-cylindrical and dispersion-free particle-in-cell algorithm. *Comput. Phys. Commun.* **2016**, *203*, 66–82. [CrossRef]
20. Hiraiwa, T.; Soutome, K.; Tanaka, H. Formulation of electron motion in a storage ring with a betatron tune varying with time and a dipole shaker working at a constant frequency. *Phys. Rev. Accel. Beams* **2021**, *24*, 114001. [CrossRef]
21. Fourmaux, S.; Hallin, E.; Chaulagain, U.; Weber, S.; Kieffer, J. Laser-based synchrotron X-ray radiation experimental scaling. *Opt. Express* **2020**, *28*, 3147–3158. [CrossRef]
22. Cole, J.M.; Symes, D.R.; Lopes, N.C.; Wood, J.C.; Poder, K.; Alatabi, S.; Botchway, S.W.; Foster, P.S.; Gratton, S.; Johnson, S.; et al. High-resolution μCT of a mouse embryo using a compact laser-driven X-ray betatron source. *Proc. Natl. Acad. Sci. USA* **2018**, *115*, 6335–6340. [CrossRef] [PubMed]
23. Kneip, S.; McGuffey, C.; Dollar, F.; Bloom, M.; Chvykov, V.; Kalintchenko, G.; Krushelnick, K.; Maksimchuk, A.; Mangles, S.; Matsuoka, T.; et al. X-ray phase contrast imaging of biological specimens with femtosecond pulses of betatron radiation from a compact laser plasma wakefield accelerator. *Appl. Phys. Lett.* **2011**, *99*, 093701. [CrossRef]
24. Fourmaux, S.; Corde, S.; Phuoc, K.T.; Lassonde, P.; Lebrun, G.; Payeur, S.; Martin, F.; Sebban, S.; Malka, V.; Rousse, A.; et al. Single shot phase contrast imaging using laser-produced Betatron X-ray beams. *Opt. Lett.* **2011**, *36*, 2426–2428. [CrossRef]
25. Guo, B.; Zhang, X.; Zhang, J.; Hua, J.; Pai, C.H.; Zhang, C.; Chu, H.H.; Mori, W.; Joshi, C.; Wang, J.; et al. High-resolution phase-contrast imaging of biological specimens using a stable betatron X-ray source in the multiple-exposure mode. *Sci. Rep.* **2019**, *9*, 7796. [CrossRef] [PubMed]
26. Elfarnawany, M.; Rohani, S.A.; Ghomashchi, S.; Allen, D.G.; Zhu, N.; Agrawal, S.K.; Ladak, H.M. Improved middle-ear soft-tissue visualization using synchrotron radiation phase-contrast imaging. *Hear. Res.* **2017**, *354*, 1–8. [CrossRef] [PubMed]
27. Gruse, J.N.; Streeter, M.; Thornton, C.; Armstrong, C.; Baird, C.; Bourgeois, N.; Cipiccia, S.; Finlay, O.; Gregory, C.; Katzir, Y.; et al. Application of compact laser-driven accelerator X-ray sources for industrial imaging. *Nucl. Instrum. Methods Phys. Res. Sect. A Accel. Spectrometers Detect. Assoc. Equip.* **2020**, *983*, 164369. [CrossRef]
28. van Tilborg, J.; Ostermayr, T.; Tsai, H.E.; Schenkel, T.; Geddes, C.; Schroeder, C.; Esarey, E. Phase-contrast imaging with laser-plasma-accelerator betatron sources. In Proceedings of the XVII International Conference on X-ray Lasers 2020, Online, 8–10 December 2020; Volume 11886, pp. 190–198.
29. Svendsen, K.; González, I.G.; Hansson, M.; Svensson, J.B.; Ekerfelt, H.; Persson, A.; Lundh, O. Optimization of soft X-ray phase-contrast tomography using a laser wakefield accelerator. *Opt. Express* **2018**, *26*, 33930–33941. [CrossRef] [PubMed]
30. Doherty, A.; Fourmaux, S.; Astolfo, A.; Ziesche, R.; Wood, J.; Finlay, O.; Stolpe, W.; Batey, D.; Manke, I.; Légaré, F.; et al. Femtosecond multimodal imaging with a laser-driven X-ray source. *Commun. Phys.* **2023**, *6*, 288. [CrossRef] [PubMed]
31. Bukreeva, I.; Mittone, A.; Bravin, A.; Festa, G.; Alessandrelli, M.; Coan, P.; Formoso, V.; Agostino, R.; Giocondo, M.; Ciuchi, F.; et al. Enhanced X-ray-phase-contrast-tomography brings new clarity to the 2000-year-old'voice'of Epicurean philosopher Philodemus. *arXiv* **2016**, arXiv:1602.08071.
32. Bukreeva, I.; Mittone, A.; Bravin, A.; Festa, G.; Alessandrelli, M.; Coan, P.; Formoso, V.; Agostino, R.G.; Giocondo, M.; Ciuchi, F.; et al. Virtual unrolling and deciphering of Herculaneum papyri by X-ray phase-contrast tomography. *Sci. Rep.* **2016**, *6*, 27227. [CrossRef]
33. Zanette, I.; Zdora, M.C.; Zhou, T.; Burvall, A.; Larsson, D.H.; Thibault, P.; Hertz, H.M.; Pfeiffer, F. X-ray microtomography using correlation of near-field speckles for material characterization. *Proc. Natl. Acad. Sci. USA* **2015**, *112*, 12569–12573. [CrossRef] [PubMed]
34. Olivo, A. Edge-illumination X-ray phase-contrast imaging. *J. Phys. Condens. Matter* **2021**, *33*, 363002. [CrossRef] [PubMed]
35. Arfelli, F.; Barbiellini, G.; Bonvicini, V.; Bravin, A.; Cantatore, G.; Castelli, E.; Di Michiel, M.; Longo, R.; Olivo, A.; Pani, S.; et al. An "edge-on" silicon strip detector for X-ray imaging. *IEEE Trans. Nucl. Sci.* **1997**, *44*, 874–880. [CrossRef]
36. Olivo, A.; Speller, R. A coded-aperture technique allowing X-ray phase contrast imaging with conventional sources. *Appl. Phys. Lett.* **2007**, *91*, 074106. [CrossRef]
37. Stutman, D.; Safca, N.; Tomassini, P.; Anghel, E.; Ur, C. Towards high-sensitivity and low-dose medical imaging with laser X-ray sources. In Proceedings of the Compact Radiation Sources from EUV to Gamma-Rays: Development and Applications, Prague, Czech Republic, 24–28 April 2023; Volume 12582, pp. 35–46.

38. Guénot, D.; Svendsen, K.; Lehnert, B.; Ulrich, H.; Persson, A.; Permogorov, A.; Zigan, L.; Wensing, M.; Lundh, O.; Berrocal, E. Distribution of liquid mass in transient sprays measured using laser-plasma-driven X-ray tomography. *Phys. Rev. Appl.* **2022**, *17*, 064056. [CrossRef]
39. Albert, F.; Lemos, N.; Shaw, J.; King, P.; Pollock, B.; Goyon, C.; Schumaker, W.; Saunders, A.; Marsh, K.; Pak, A.; et al. Betatron X-ray radiation in the self-modulated laser wakefield acceleration regime: Prospects for a novel probe at large scale laser facilities. *Nucl. Fusion* **2018**, *59*, 032003. [CrossRef]
40. Mahieu, B.; Jourdain, N.; Ta Phuoc, K.; Dorchies, F.; Goddet, J.P.; Lifschitz, A.; Renaudin, P.; Lecherbourg, L. Probing warm dense matter using femtosecond X-ray absorption spectroscopy with a laser-produced betatron source. *Nat. Commun.* **2018**, *9*, 3276. [CrossRef] [PubMed]
41. Dorchies, F.; Ta Phuoc, K.; Lecherbourg, L. Nonequilibrium warm dense matter investigated with laser–plasma-based XANES down to the femtosecond. *Struct. Dyn.* **2023**, *10*, 054301. [CrossRef]
42. Grolleau, A.; Dorchies, F.; Jourdain, N.; Phuoc, K.T.; Gautier, J.; Mahieu, B.; Renaudin, P.; Recoules, V.; Martinez, P.; Lecherbourg, L. Femtosecond Resolution of the Nonballistic Electron Energy Transport in Warm Dense Copper. *Phys. Rev. Lett.* **2021**, *127*, 275901. [CrossRef]
43. Principi, E.; Giangrisostomi, E.; Mincigrucci, R.; Beye, M.; Kurdi, G.; Cucini, R.; Gessini, A.; Bencivenga, F.; Masciovecchio, C. Extreme ultraviolet probing of nonequilibrium dynamics in high energy density germanium. *Phys. Rev. B* **2018**, *97*, 174107. [CrossRef]
44. Principi, E.; Krylow, S.; Garcia, M.; Simoncig, A.; Foglia, L.; Mincigrucci, R.; Kurdi, G.; Gessini, A.; Bencivenga, F.; Giglia, A.; et al. Atomic and electronic structure of solid-density liquid carbon. *Phys. Rev. Lett.* **2020**, *125*, 155703. [CrossRef] [PubMed]
45. Le Guyader, L.; Eschenlohr, A.; Beye, M.; Schlotter, W.; Döring, F.; Carinan, C.; Hickin, D.; Agarwal, N.; Boeglin, C.; Bovensiepen, U.; et al. Photon-shot-noise-limited transient absorption soft X-ray spectroscopy at the European XFEL. *J. Synchrotron Radiat.* **2023**, *30*, 284–300. [CrossRef] [PubMed]
46. Mo, M.; Chen, Z.; Fourmaux, S.; Saraf, A.; Kerr, S.; Otani, K.; Masoud, R.; Kieffer, J.C.; Tsui, Y.; Ng, A.; et al. Measurements of ionization states in warm dense aluminum with betatron radiation. *Phys. Rev. E* **2017**, *95*, 053208. [CrossRef] [PubMed]
47. Kettle, B.; Gerstmayr, E.; Streeter, M.; Albert, F.; Baggott, R.; Bourgeois, N.; Cole, J.; Dann, S.; Falk, K.; González, I.G.; et al. Single-shot multi-keV X-ray absorption spectroscopy using an ultrashort laser-wakefield accelerator source. *Phys. Rev. Lett.* **2019**, *123*, 254801. [CrossRef] [PubMed]
48. Kettle, B.; Colgan, C.; Los, E.; Gerstmayr, E.; Streeter, M.; Albert, F.; Astbury, S.; Baggott, R.; Cavanagh, N.; Falk, K.; et al. X-ray absorption spectroscopy using an ultrafast laboratory-scale laser-plasma accelerator source. *arXiv* **2023**, arXiv:2305.10123.
49. Raclavskỳ, M.; Khakurel, K.P.; Chaulagain, U.; Lamač, M.; Nejdl, J. Multi-lane mirror for broadband applications of the betatron X-ray source. *Photonics* **2021**, *8*, 579. [CrossRef]
50. Zeraouli, G.; Gatti, G.; Longman, A.; Pérez-Hernández, J.; Arana, D.; Batani, D.; Jakubowska, K.; Volpe, L.; Roso, L.; Fedosejevs, R. Development of an adjustable Kirkpatrick-Baez microscope for laser driven X-ray sources. *Rev. Sci. Instrum.* **2019**, *90*, 063704. [CrossRef] [PubMed]
51. Gurman, S. Interpretation of EXAFS data. *J. Synchrotron Radiat.* **1995**, *2*, 56–63. [CrossRef]
52. Henderson, G.S.; De Groot, F.M.; Moulton, B.J. X-ray absorption near-edge structure (XANES) spectroscopy. *Rev. Mineral. Geochem.* **2014**, *78*, 75–138. [CrossRef]